An efficient self-consistent field method for large systems of weakly interacting components

Rustam Z. Khaliullin[a)]
Department of Chemistry, University of California Berkeley, California 94720

Martin Head-Gordon[b)]
Department of Chemistry, University of California Berkeley, California 94720 and Chemical Sciences Division, Lawrence Berkeley National Laboratory, Berkeley, California 94720

Alexis T. Bell[c)]
Chemical Sciences Division, Lawrence Berkeley National Laboratory, Berkeley, California 94720 and Department of Chemical Engineering, University of California Berkeley, California 94720

(Received 21 December 2005; accepted 7 March 2006; published online 23 May 2006)

An efficient method for removing the self-consistent field (SCF) diagonalization bottleneck is proposed for systems of weakly interacting components. The method is based on the equations of the locally projected SCF for molecular interactions (SCF MI) which utilize absolutely localized nonorthogonal molecular orbitals expanded in local subsets of the atomic basis set. A generalization of direct inversion in the iterative subspace for nonorthogonal molecular orbitals is formulated to increase the rate of convergence of the SCF MI equations. Single Roothaan step perturbative corrections are developed to improve the accuracy of the SCF MI energies. The resulting energies closely reproduce the conventional SCF energy. Extensive test calculations are performed on water clusters up to several hundred molecules. Compared to conventional SCF, speedups of the order of $(N/O)^2$ have been achieved for the diagonalization step, where N is the size of the atomic orbital basis, and O is the number of occupied molecular orbitals. © *2006 American Institute of Physics*. [DOI: 10.1063/1.2191500]

I. INTRODUCTION

Weakly bonded molecular complexes represent a broad class of systems with interesting chemical and physical properties. Intermolecular forces determine many important properties of liquids and solutions, and govern physisorption in van der Waals systems.[1] They also control self-assembly and self-organization processes in supramolecular systems such as supramolecular polymers and liquid crystals.[2] Hydrogen bonding, one of the most abundant types of intermolecular interactions, plays an important role in the chemistry of numerous systems, ranging from small water clusters to nanodroplets, and finally bulk water, as well as solvated biomolecules.[3,4] Because of their broad importance, there is considerable interest in developing theoretical approaches for describing interactions of weakly bonded ensembles of molecules.

First principles electronic structure methods are already playing an important role in the study of molecular clusters and liquids. Their applications range from high accuracy calculations on small- to medium-sized clusters[5–7] to more approximate calculations of dynamics of molecules in the condensed phase.[8,9] The building block for virtually all electronic structure methods is the self-consistent field (SCF) model,[10] which is the basis of all Kohn-Sham density functional theory (DFT) models,[11] as well as Hartree–Fock-based molecular orbital theory.[10] From the computational standpoint, SCF calculations involve two computationally significant steps that are repeated on each iteration. First is the assembly of the effective Hamiltonian (or Fock operator) for the current set of molecular orbitals. Second is the diagonalization of this Fock operator in an orthogonalized basis to yield an improved set of molecular orbitals.

Developing efficient algorithms for both of these steps has attracted much attention over the past decade. Advances in methods for the formation of the Coulomb,[12–17] exact exchange,[18,19] and exchange-correlation[20,21] parts of the Fock matrix have made it possible to achieve linear scaling with a relatively low prefactor for this part of the SCF procedure. Thus, the diagonalization of the Fock matrix, which scales cubically with the system size, becomes the bottleneck for calculations for large systems.[22] A number of alternative methods have been proposed for updating the molecular orbitals (or the one-particle density matrix) which are capable of yielding linear scaling.[23–25] However, for dense three-dimensional systems, these methods become effective only for very large system sizes, because they depend upon orbital localization which requires length scales of roughly ten atoms in a line (i.e., on the order of 1000's of atoms).[23,26] This is too large for routine use at present.

It is also possible to consider customizing the SCF procedure for particular physical systems, either for physical or computational advantage. The importance of intermolecular interactions has motivated the development of several modified SCF methods for weakly bonded systems.[27–30] These

[a)]Electronic mail: rustam@khaliullin.com
[b)]Electronic mail: m_headgordon@berkeley.edu
[c)]Electronic mail: alexbell@berkeley.edu

methods focus primarily on an *a priori* elimination of the basis set superposition error (BSSE) from the interaction energy between fragments. All proposed formulations are based on expansion of molecular orbitals (MOs) in local subsets of atomic orbitals (AOs). Such an expansion leads to absolutely localized MOs (ALMOs) for which the only computational disadvantage is their nonorthogonality. Stoll *et al.*[31] were the first to generalize the SCF equations for the nonorthogonal ALMOs. All other authors have used equivalent equations in their BSSE-free methods. As proposed by Nagata *et al.*,[29] such schemes will be referred to as locally projected self-consistent field for molecular interactions (LP SCF MI) or, simply, SCF MI. In this work, we first show how the utilization of the SCF MI equations replaces diagonalization with a procedure that has better scaling properties and reduces computational time significantly even for systems of moderate size. A concise derivation of the SCF MI equations is presented in Sec. II.

It is known that the iterative procedure for solving SCF equations is slow without a proper acceleration scheme. Direct inversion in the iterative subspace (DIIS),[32,33] the most successful acceleration scheme for the SCF method, cannot be used for SCF MI without proper generalization for the case of nonorthogonal MOs. We next show how the equation for the Pulay DIIS error vector can be generalized for the case of ALMOs so as to enable efficient solution of the SCF MI equations. The DIIS scheme presented here is a useful alternative to the DIIS-accelerated SCF MI method proposed previously.[34] The DIIS error vector equation derived in this paper reproduces the conventional Pulay equation if the locality constraint on MOs is lifted. It also enables faster evaluation of the error vector than the equation used previously.

As have been shown by Hamza *et al.*,[35] confinement of MOs to a fragment leads to an underestimation of the binding energies between the fragments (it is a constraint upon the interacting fragments, that has no effect when they are noninteracting). However, this error can be reduced using perturbation theory. Nagata and Iwata[36] have proposed inclusion of a perturbative correction by calculating Hamiltonian elements between the ground SCF MI wave function and singly excited wave functions. They demonstrated that this method gives the binding energies that are very close to the full SCF energies for water dimer. However, the formalism behind their method is somewhat involved and the resulting locally projected single excitation second-order Moller-Plesset (LP SE MP2) perturbation method is not readily applicable to large systems. Here, we present an alternative perturbative correction scheme that scales cubically with the size of the system and test it on water clusters to show that the final results are close to those obtained from full SCF calculations.

Therefore, this paper describes modifications and improvements to the original SCF MI method that make it practical for calculations on the Hartree–Fock (HF)/DFT level for large closed-shell systems of weakly interacting closed-shell fragments.

II. THEORY

The following notation is used throughout the paper. u–z: fragment indices, Greek letters: AO indices, i–m: occupied MO indices, a and b: virtual MO indices, p and q: generic MO indices, $|\phi_{x\mu}\rangle$: AO localized on fragment x, $|\psi_{xi}\rangle$: spatial MO localized on fragment x, N: total number of AOs in the system, O: total number of doubly occupied MOs in the system, V: total number of virtual spatial MOs in the system, F: number of fragments, n_x: number of AOs on fragment x, o_x: number of doubly occupied MOs on fragment x, v_x: number of virtual spatial MOs on fragment x, $o=\max_{x\in 1\cdots F}(o_x)$, $n=\max_{x\in 1\cdots F}(n_x)$, $v=\max_{x\in 1\cdots F}(v_x)$.

We use tensor algebra to work with the nonorthogonal atomic basis set.[37] There is one important exception, however, which is that the Einstein convention does not imply summation over fragment indices.

A. SCF MI equations

In the first step, the atoms and the electrons of the entire system are logically divided into nonoverlapping subsets. These subsets are referred to as fragments, and each fragment must contain a specified integer number of electrons. To meet this definition, each fragment must represent a part that interacts weakly with the rest of the system. For example, in molecular clusters the boundaries between the fragments must not cross covalent bonds in the molecules.

It is worth noting that such a division scheme uses natural partitioning of the system. It does not rely on any distance cut-off thresholds and, therefore, produces smooth potential energy surfaces as long as fragments retain their chemical identity. Within this restriction, it satisfies the requirements of a well-defined theoretical model chemistry.[38] Upon the division the AOs localized on the atoms also become partitioned into subsets $\{|\phi_{x\mu}\rangle\}$, where the first index denotes a subset and the second is the number of the basis function within the given subset.

In the next step, the occupied MOs on a fragment are expanded in terms of AOs of the same fragment,

$$|\psi_{xi}\rangle = |\phi_{x\mu}\rangle T^{x\mu}_{\cdot\cdot xi}, \tag{1}$$

where the MO coefficients $T^{x\mu}_{\cdot\cdot yi}$ are constrained to be zero for $x\neq y$. These constraints produce MOs that are localized on fragments in the same sense as AOs are localized on atoms. Thus, such MOs are called absolutely localized MOs. Expansion (1) excludes charge transfer from one fragment to another, which is undesirable, as this is a physical effect that can play a role in phenomena such as hydrogen bonding. It also prevents electrons on one fragment from borrowing the atomic orbitals of other fragments to compensate for incompleteness of their own AOs, which is desirable, since this basis set superposition effect will unphysically lower the interaction energy.

The constrained MOs are not orthogonal from one fragment to the next (imposing such orthogonality would be an additional constraint that cannot be physically justified). Their overlap is described by the covariant σ matrix,

$$\sigma_{yj,xi} = \langle \psi_{yj} | \psi_{xi} \rangle, \tag{2}$$

and the inverse overlap is the contravariant σ^{-1} matrix,

$$\sigma^{yj,xi} \equiv (\sigma^{-1})_{yj,xi}. \tag{3}$$

The electronic HF energy of a closed-shell determinant is

$$E = \sum_{x}^{F} \langle \psi_{xi} | \hat{h} + \hat{f} | \psi^{xi} \rangle, \tag{4}$$

where the core Hamiltonian $\hat{h}$ and the Fock operator $\hat{f}$ have their usual definitions and the contravariant MOs $|\psi^{xi}\rangle$ are defined as

$$|\psi^{xi}\rangle = \sum_{y}^{F} |\psi_{yj}\rangle \sigma^{yj,xi}. \tag{5}$$

Stoll *et al.*[31] have shown that the variation of E with respect to the occupied MOs $|\psi_{xi}\rangle$ is given by

$$\delta E = 4 \langle \delta \psi_{xi} | (\hat{1} - \hat{\rho}) \hat{f} | \psi^{xi} \rangle, \tag{6}$$

where $\hat{\rho}$ is the one-particle density operator,

$$\hat{\rho} = \sum_{x}^{F} |\psi^{xi}\rangle \langle \psi_{xi}|. \tag{7}$$

Therefore, the necessary condition for a minimum of the energy with constraints (1) is

$$(\hat{1} - \hat{\rho}) \hat{f} | \psi^{xi} \rangle = 0. \tag{8}$$

Equation (8) is the generalized SCF equation. It degenerates to the conventional SCF equation in the case of orthonormal MOs,

$$\hat{f} | \psi_{xi} \rangle = | \psi_{xi} \rangle \epsilon_{xi}, \tag{9}$$

where the matrix elements $\langle \psi_{yj} | \hat{f} | \psi_{xi} \rangle$ are assumed to be $\epsilon_{xi} \delta_{yj,xi}$.

For partitioned systems, Eq. (8) can also be cast into an eigenvalue form using a Hermitian operator for each fragment x,

$$\hat{\rho}^{x} = |\psi^{xi}\rangle \langle \psi^{xi}|, \tag{10}$$

that by definition has the property,

$$\hat{\rho}^{x} | \psi_{xi} \rangle = | \psi^{xi} \rangle. \tag{11}$$

The left-hand side of Eq. (8) then may be rewritten as follows:

$$(\hat{1} - \hat{\rho} + \hat{\rho}^{x}) \hat{f} | \psi^{xi} \rangle - \hat{\rho}^{x} \hat{f} | \psi^{xi} \rangle = (\hat{1} - \hat{\rho} + \hat{\rho}^{x}) \hat{f} (\hat{1} - \hat{\rho} + \hat{\rho}^{x}) | \psi_{xi} \rangle - | \psi^{xj} \rangle \langle \psi^{xj} | \hat{f} | \psi^{xi} \rangle. \tag{12}$$

As in the conventional HF equation, it can be assumed that $\langle \psi^{xj} | \hat{f} | \psi^{xi} \rangle = \langle \psi_{xj} | \hat{f}^{x}_{G} | \psi_{xi} \rangle = \epsilon_{xi} \delta_{ij}$. Thus, Eq. (8) now reads as

$$\hat{f}^{x}_{G} | \psi_{xi} \rangle = (\hat{1} - \hat{\rho} + \hat{\rho}^{x}) | \psi_{xi} \rangle \epsilon_{xi}, \tag{13}$$

with the projected Fock operator,

$$\hat{f}^{x}_{G} \equiv (\hat{1} - \hat{\rho} + \hat{\rho}^{x}) \hat{f} (\hat{1} - \hat{\rho} + \hat{\rho}^{x}). \tag{14}$$

The AO representation of Eq. (13) gives the matrix equation (23) that reproduces equations published by Gianinetti *et al.*[27,28] without derivation.

Stoll *et al.*[31] have derived a similar equation in the same way but using a non-Hermitian equivalent of the fragment density operator,

$$\hat{s}^{x} = |\psi^{xi}\rangle \langle \psi_{xi}|, \tag{15}$$

and assuming (without loss of generality) that the MOs are orthogonal within a fragment. The final Stoll equation has the form

$$\hat{f}^{x}_{S} | \psi_{xi} \rangle = | \psi_{xi} \rangle \epsilon_{xi}, \tag{16}$$

with a different projected Fock operator,

$$\hat{f}^{x}_{S} \equiv (\hat{1} - \hat{\rho} + \hat{s}^{x\dagger}) \hat{f} (\hat{1} - \hat{\rho} + \hat{s}^{x}). \tag{17}$$

It can be derived from Eq. (8) using the following properties of $\hat{s}^{x}$:

$$\hat{s}^{x} | \psi^{yi} \rangle = \delta_{xy} | \psi^{yi} \rangle, \tag{18}$$

$$\hat{s}^{x} | \psi_{xi} \rangle = | \psi^{xi} \rangle. \tag{19}$$

A projected equation of a slightly different form was used by Nagata *et al.*[29,36]

$$\hat{f}^{x}_{N} | \psi_{xi} \rangle = (\hat{1} - \hat{p}^{\ominus x}) | \psi_{xi} \rangle \epsilon_{xi}, \tag{20}$$

where

$$\hat{f}^{x}_{N} \equiv (\hat{1} - \hat{p}^{\ominus x}) \hat{f} (\hat{1} - \hat{p}^{\ominus x}), \tag{21}$$

$$\hat{p}^{\ominus x} \equiv \sum_{y \neq x}^{F} \sum_{z \neq x}^{F} |\psi_{yj}\rangle (\sigma_{\ominus x})^{yj,zk} \langle \psi_{zk}|. \tag{22}$$

These equations can also be derived from (8) with the assumption that the diagonal blocks of the inverse MO overlap are unit matrices. The detailed derivation can be found in the original paper.[36]

Multiplying Eqs. (13), (16), and (20) by $\langle \phi_{x\mu}|$ from the left one gets the matrix equations

$$[\mathbf{f}^{x}_{A}]_{xx} [\mathbf{T}]_{xx} = [\mathbf{S}^{x}_{A}]_{xx} [\mathbf{T}]_{xx} [\boldsymbol{\epsilon}]_{xx}. \tag{23}$$

Here, the fragment Fock matrix elements, $(\mathbf{f}^{x}_{A})_{x\mu,x\nu} \equiv \langle \phi_{x\mu} | \hat{f}^{x}_{A} | \phi_{x\nu} \rangle$, are matrix elements of the corresponding projected Fock operators $\hat{f}^{x}_{A}$, where $A = G, S, N$ for the formulations of Gianinetti, Stoll, and Nagata, respectively. The fragment overlap matrix elements are defined as $\mathbf{S}^{x}_{x\mu,x\nu} \equiv \langle \phi_{x\mu} | (\hat{1} - \hat{\rho} + \hat{\rho}^{x}) | \phi_{x\nu} \rangle$ for the Gianinetti equations, $\mathbf{S}^{x}_{x\mu,x\nu} \equiv \mathbf{S}_{x\mu,x\nu}$ for the Stoll equations, and $\mathbf{S}^{x}_{x\mu,x\nu} \equiv \langle \phi_{x\mu} | (\hat{1} - \hat{p}^{\ominus x}) | \phi_{x\nu} \rangle$ for the Nagata equations. The eigenvalue matrix $\boldsymbol{\epsilon}$ is an $N \times N$ diagonal matrix, and $[\ldots]_{xy}$ denotes xth, yth block.

We have already emphasized that the locally projected formulation of the SCF equations excludes BSSE and charge-transfer effects. From a computational standpoint, it is now clear that the main accomplishment of Eq. (23) is the

replacement of the diagonalization of the full $N\times N$ Fock matrix $\mathbf{f}$ with separate diagonalizations of F projected Fock matrices $\mathbf{f}^x$ $(n_x\times n_x)$, one for each fragment. As will be shown below this leads to a significant speedup in the MO update routine in the SCF iterations. Computational aspects of the approaches of Gianinetti, Stoll, and Nagata will be compared in Sec. III.

B. DIIS error vector

In the case of the orthogonal MOs a new idempotent density operator $\hat{\rho}$ may be obtained as a unitary transformation $\hat{U}$ of the initial operator $\hat{\rho}_0$. The unitary transformation $\hat{U}$ can be parametrized by an anti-Hermitian operator $\hat{\Delta}$,

$$\hat{\rho}=\sum_{i}^{O}\hat{U}|\psi_i^0\rangle\langle\psi_i^0|\hat{U}^\dagger=e^{-\hat{\Delta}}\hat{\rho}_0e^{\hat{\Delta}}\approx\hat{\rho}_0-\hat{\Delta}\hat{\rho}_0+\hat{\rho}_0\hat{\Delta}. \tag{24}$$

The infinitesimally small transformation of the density matrix in the atomic orbital "covariant integral representation"[39] is

$$\tilde{R}^{\lambda\sigma}=\langle\phi^\lambda|\hat{\rho}|\phi^\sigma\rangle=R^{\lambda\sigma}-\Delta^{\lambda\nu}S_{\nu\mu}R^{\mu\sigma}+R^{\lambda\nu}S_{\nu\mu}\Delta^{\mu\sigma}. \tag{25}$$

The DIIS error vector is usually given by the derivative of the total electronic energy,

$$E=\tilde{R}^{\lambda\sigma}(h_{\sigma\lambda}+\tilde{f}_{\sigma\lambda}), \tag{26}$$

with respect to the parameters $\Delta^{\rho\tau}$,

$$(\mathrm{err})_{\tau\rho}\equiv\left.\frac{\partial E}{\partial\Delta^{\rho\tau}}\right|_{\Delta=0}=\left.\frac{\partial E}{\partial\tilde{R}^{\lambda\sigma}}\frac{\partial\tilde{R}^{\lambda\sigma}}{\partial\Delta^{\rho\tau}}\right|_{\Delta=0}=2f_{\sigma\lambda}\left.\frac{\partial\tilde{R}^{\lambda\sigma}}{\partial\Delta^{\rho\tau}}\right|_{\Delta=0}$$
$$=2(f_{\tau\lambda}R^{\lambda\sigma}S_{\sigma\rho}-S_{\tau\lambda}R^{\lambda\sigma}f_{\sigma\rho}). \tag{27}$$

A nonsingular operator $\hat{V}$, which is not necessarily unitary, transforms the orbitals in the case of the nonorthogonal MOs. The infinitesimally small transformation can be expanded in terms of operator $\hat{\Delta}$ as $\hat{V}=\hat{1}-\hat{\Delta}$ ignoring the higher-order terms in $\hat{\Delta}$. Transformation $\hat{V}$ must preserve the block-diagonal structure of $\mathbf{T}$ and, therefore, $\hat{\Delta}$ is represented as

$$\hat{\Delta}=\sum_{x}^{F}\hat{\Delta}^x, \tag{28}$$

with

$$\hat{\Delta}^x=|\phi_{x\mu}\rangle\Delta^{x\mu,x\sigma}S_{x\sigma,x\nu}\langle\phi^{x\nu}| \tag{29}$$

and

$$\hat{\Delta}^{x\dagger}=-|\phi^{x\nu}\rangle S_{x\nu,x\sigma}\Delta^{x\sigma,x\mu}\langle\phi_{x\mu}|. \tag{30}$$

The infinitesimally transformed density operator is

$$\hat{\rho}=\sum_{x,y}^{F}(\hat{1}-\hat{\Delta}^x)|\psi_{xi}^0\rangle(\sigma(\hat{\Delta}))^{xi,yj}\langle\psi_{yj}^0|(\hat{1}-\hat{\Delta}^{y\dagger}), \tag{31}$$

and, therefore, the transformed density matrix in the covariant integral representation is

$$\tilde{R}^{z\lambda,w\sigma}=\langle\phi^{z\lambda}|\hat{\rho}|\phi^{w\sigma}\rangle$$
$$=(T_{\cdot\,zi}^{z\lambda\,\cdot}-\Delta^{z\lambda,z\pi}S_{z\pi,z\nu}T_{\cdot\,zi}^{z\lambda\,\cdot})(\sigma(\Delta))^{zi,wj}$$
$$\times(T_{wj\,\cdot}^{\cdot\,w\sigma}+T_{wj\,\cdot}^{\cdot\,w\nu}S_{w\nu,w\pi}\Delta^{w\pi,w\sigma}), \tag{32}$$

with the MO overlap matrix σ changing as a function of $\hat{\Delta}$,

$$\sigma(\Delta)_{ul,yp}=\langle\psi_{ul}^0|(\hat{1}-\hat{\Delta}^{u\dagger}-\hat{\Delta}^y)|\psi_{yp}^0\rangle$$
$$=\sigma_{ul,yp}+T_{ul\,\cdot}^{\cdot\,u\nu}S_{u\nu,u\sigma}\Delta^{u\sigma,u\mu}T_{u\mu,yp}$$
$$-T_{ul,y\mu}\Delta^{y\mu,y\sigma}S_{y\sigma,y\nu}T_{\cdot\,yp}^{y\nu\,\cdot}. \tag{33}$$

Just as in (27), the DIIS error matrix is defined as the derivative of the energy (26) with respect to parameters $\Delta^{x\rho,x\tau}$,

$$(\mathrm{err})_{x\tau,x\rho}\equiv\left.\frac{\partial E}{\partial\Delta^{x\rho,x\tau}}\right|_{\Delta=0}=\sum_{z,w}^{F}\left.\frac{\partial E}{\partial\tilde{R}^{z\lambda,w\sigma}}\frac{\partial\tilde{R}^{z\lambda,w\sigma}}{\partial\Delta^{x\rho,x\tau}}\right|_{\Delta=0}$$
$$=\sum_{z,w}^{F}2f_{w\sigma,z\lambda}\left.\frac{\partial\tilde{R}^{z\lambda,w\sigma}}{\partial\Delta^{x\rho,x\tau}}\right|_{\Delta=0}, \tag{34}$$

$$\left.\frac{\partial\tilde{R}^{z\lambda,w\sigma}}{\partial\Delta^{x\rho,x\tau}}\right|_{\Delta=0}=\delta_{wx}\delta_{\tau\sigma}R^{z\lambda,w\nu}S_{w\nu,x\rho}-\delta_{zx}\delta_{\rho\lambda}S_{x\tau,z\nu}R^{z\nu,w\sigma}$$
$$+T_{\cdot\,zi}^{z\lambda\,\cdot}\left.\frac{\partial(\sigma(\Delta))^{zi,wj}}{\partial\Delta^{x\rho,x\tau}}\right|_{\Delta=0}T_{wj\,\cdot}^{\cdot\,w\sigma}, \tag{35}$$

$$\left.\frac{\partial(\sigma(\Delta))^{zi,wj}}{\partial\Delta^{x\rho,x\tau}}\right|_{\Delta=0}=-\sum_{u,y}^{F}\sigma^{zi,ul}\left.\frac{\partial(\sigma(\Delta))_{ul,ym}}{\partial\Delta^{x\rho,x\tau}}\right|_{\Delta=0}\sigma^{ym,wj}, \tag{36}$$

$$\left.\frac{\partial(\sigma(\Delta))_{ul,ym}}{\partial\Delta^{x\rho,x\tau}}\right|_{\Delta=0}=\delta_{ux}T_{ul\,\cdot}^{\cdot\,u\nu}S_{u\nu,x\rho}T_{u\tau,ym}$$
$$-\delta_{yx}T_{ul,y\rho}S_{x\tau,y\nu}T_{\cdot\,ym}^{y\nu\,\cdot}. \tag{37}$$

Combining Eqs. (34)–(37) one obtains

$$(\mathrm{err})_{x\tau,x\rho}=2\Bigg(\sum_{z}^{F}f_{x\tau,z\lambda}R^{z\lambda,x\nu}S_{x\nu,x\rho}-\sum_{z}^{F}S_{x\tau,x\nu}R^{x\nu,z\lambda}f_{z\lambda,x\rho}$$
$$+\sum_{z,w,y}^{F}S_{x\tau,x\nu}R^{x\nu,z\lambda}f_{z\lambda,w\sigma}R^{w\sigma,y\pi}S_{y\pi,x\rho}$$
$$-\sum_{z,w,y}^{F}S_{x\tau,y\pi}R^{y\pi,w\omega}f_{w\omega,z\lambda}R^{z\lambda,x\nu}S_{x\nu,x\rho}\Bigg), \tag{38}$$

or, in matrix notation,

$$[\mathrm{err}]_{xx}=2[\mathbf{S}]_{xx}[\mathbf{Rf}(\mathbf{RS}-\mathbf{1})]_{xx}-2[(\mathbf{SR}-\mathbf{1})\mathbf{fR}]_{xx}[\mathbf{S}]_{xx}. \tag{39}$$

Equation (38) becomes Eq. (27) in the limit of infinite separation between the fragments. As Eq. (38) suggests, the number of parameters in the error vector is reduced from N^2 to $\Sigma_x^F n_x^2$. Thus, the computation of the DIIS error can be performed faster (see Secs. III and IV) than in the conventional SCF.

Equation (38) can also be used in the curvy steps minimization of the total energy with ALMOs.[39]

C. Perturbative correction of the converged SCF MI

The SCF MI energy with the block-diagonal constraints (1) on the variational degrees of freedom is always higher than the full SCF energy. It has been shown[35] that the full SCF binding energies between fragments cannot be reproduced accurately with this approximation even in large basis sets. The perturbation theory developed here brings the SCF MI energies much closer to the full SCF result.

The exact one-electron Hamiltonian is chosen as the full SCF Fock operator $\hat{f}(\hat{\rho}_{\mathrm{MI}})$ for the cluster, where $\hat{\rho}_{\mathrm{MI}}$ is the converged SCF MI density operator. This one-electron Hamiltonian is of course different from the converged cluster one-electron Hamiltonian $\hat{f}(\hat{\rho}_{\mathrm{SCF}})$, which is built from the fully converged supermolecule density $\hat{\rho}_{\mathrm{SCF}}$. However, the only cases for which perturbation results are valid are the cases in which $\hat{\rho}_{\mathrm{MI}}$ is close to $\hat{\rho}_{\mathrm{SCF}}$. Therefore, $\hat{f}(\hat{\rho}_{\mathrm{MI}})$ is a good representation of the fully converged cluster Fock operator $\hat{f}(\hat{\rho}_{\mathrm{SCF}})$. Indeed, test calculations show the perturbative expansion with $\hat{f}(\hat{\rho}_{\mathrm{MI}})$ as the Hamiltonian converges and gives good agreement with the full SCF result.

The zeroth-order Hamiltonian is taken as

$$\hat{f}_0(\hat{\rho}_{\mathrm{MI}}) = \hat{\rho}_{\mathrm{MI}}\hat{f}(\hat{\rho}_{\mathrm{MI}})\hat{\rho}_{\mathrm{MI}} + (\hat{1} - \hat{\rho}_{\mathrm{MI}})\hat{f}(\hat{\rho}_{\mathrm{MI}})(\hat{1} - \hat{\rho}_{\mathrm{MI}}). \quad (40)$$

Orthonormal orbitals that diagonalize $\hat{f}_0(\hat{\rho}_{\mathrm{MI}})$ can be constructed by mixing the occupied ALMOs among themselves and by mixing the virtual ALMOs among themselves,

$$|\bar{\psi}_i\rangle = \sum_x^F \sum_j^{o_x} |\psi_{xj}\rangle K_{xj,i}, \quad (41)$$

$$|\bar{\psi}_a\rangle = \sum_x^F \sum_j^{v_x} |\psi_{xj}\rangle K_{xj,a}. \quad (42)$$

The coefficients $K_{xj,p}$ are such that $\langle\bar{\psi}_p|\hat{f}_0(\hat{\rho}_{\mathrm{MI}})|\bar{\psi}_q\rangle = \delta_{pq}\bar{\epsilon}_p$. Clearly, the orbitals $|\bar{\psi}_q\rangle$ span the same occupied and virtual subspaces as the converged nonorthogonal ALMOs. However, the orbitals $|\bar{\psi}_q\rangle$ are not localized on single fragments anymore and are orthonormal.

The one-electron perturbation operator is written as

$$\hat{v}(\hat{\rho}_{\mathrm{MI}}) = \hat{\rho}_{\mathrm{MI}}\hat{f}(\hat{\rho}_{\mathrm{MI}})(\hat{1} - \hat{\rho}_{\mathrm{MI}}) + \hat{\rho}_{\mathrm{MI}}\hat{f}(\hat{\rho}_{\mathrm{MI}})(\hat{1} - \hat{\rho}_{\mathrm{MI}}). \quad (43)$$

$\hat{v}(\hat{\rho}_{\mathrm{MI}})$ has zero occupied-occupied and virtual-virtual blocks in the $|\bar{\psi}_q\rangle$ basis by construction. Using standard perturbation theory with $\hat{f}_0(\hat{\rho}_{\mathrm{MI}})$ and $\hat{v}(\hat{\rho}_{\mathrm{MI}})$ one obtains the following expression for the energy corrections:

$$E^{(1)} = 0,$$

$$E^{(2)} = 2\sum_i^O \epsilon_i^{(2)} = 2\sum_i^O \sum_a^V \frac{\bar{f}_{ia}^2}{\bar{\epsilon}_i - \bar{\epsilon}_a},$$

$$E^{(3)} = 0, \quad (44)$$

$$E^{(4)} = 2\sum_i^O \sum_a^V \sum_b^V \sum_{j\neq i}^O \frac{\bar{f}_{ia}\bar{f}_{aj}\bar{f}_{jb}\bar{f}_{bi}}{(\bar{\epsilon}_i - \bar{\epsilon}_a)(\bar{\epsilon}_i - \bar{\epsilon}_j)(\bar{\epsilon}_i - \bar{\epsilon}_b)} - 2\sum_i^O \epsilon_i^{(2)} \sum_a^V \frac{\bar{f}_{ia}^2}{(\bar{\epsilon}_i - \bar{\epsilon}_a)^2},$$

where $\bar{f}_{ia} = \langle\bar{\psi}_i|\hat{f}(\hat{\rho}_{\mathrm{MI}})|\bar{\psi}_a\rangle$.

The correction for the orbitals is

$$|\bar{\psi}_i^{(1)}\rangle = \sum_a^V |\bar{\psi}_a\rangle \frac{\bar{\phi}_{ai}}{\bar{\epsilon}_i - \bar{\epsilon}_a}. \quad (45)$$

The second-order energy correction gives the same energy lowering as an approximate Roothaan step based on the gradient of the energy with respect to the occupied-virtual coupling parameters.[40,41] From the configuration point of view, Eq. (44) corresponds to the second-order correction from non-Brillouin singles and is equivalent to the LP SE MP2 correction proposed by Nagata and Iwata.[36] The formalism presented here is different from the original LP SE MP2. We have chosen to use pseudocanonical orthogonal delocalized MOs $|\bar{\psi}_q\rangle$ in order to avoid dealing with the nonorthogonal singly excited determinants constructed from ALMOs. The downside of the simplicity of our formalism is the delocalization of the MOs $|\bar{\psi}_q\rangle$. The perturbative method developed here is referred to as locally projected SCF for molecular interactions with approximate single Roothaan step perturbative correction or SCF MI(ARS).

Correction of the infinite order can be obtained by a diagonalization of the $\hat{f}(\hat{\rho}_{\mathrm{MI}})$ matrix in the AO basis. This approach is closely related to the single Roothaan step correction in dual-basis set calculations[40] and, therefore, referred to as SCF MI(RS). The energy correction in this case is

$$E^{(\infty)} = 2\,\mathrm{Tr}\,\hat{f}(\hat{\rho}_{\mathrm{MI}})(\hat{\rho}_\infty - \hat{\rho}_{\mathrm{MI}}), \quad (46)$$

where $\hat{\rho}_\infty$ is the density constructed from the orbitals obtained from the full diagonalization of $\hat{f}(\hat{\rho}_{\mathrm{MI}})$ in the AO basis.

Convergence of the perturbation expansion together with computational efficiency of both SCF MI(ARS) and SCF MI(RS) methods will be discussed in Sec. IV.

III. IMPLEMENTATION

The SCF MI, SCF MI(ARS), and SCF MI(RS) algorithms were implemented in a development version of the Q-CHEM software package.[42] This section describes the scaling properties of these algorithms.

A. SCF MI algorithm

Several components of a conventional SCF algorithm must be modified to perform the SCF MI calculations. First, the initial guess at the MO coefficients must satisfy the block-diagonal constraints (1). Second, the evaluation of the density matrix requires the inverse of the ALMO overlap matrix. Third, the generalized DIIS error vector (38) is calculated in place of the conventional DIIS error vector (27).

Finally, the diagonalization of the full Fock matrix is replaced with the construction and diagonalization of F effective locally projected Fock matrices.

The initial guess at the density matrix was constructed from the superposition of the converged MOs on isolated fragments. MOs on a fragment can be converged in time proportional to n^3. Thus, the formation of the initial guess for the cluster scales as $Fnnn$ (i.e., linearly with system size).

The one-electron density matrix produced from the nonorthogonal orbitals is evaluated as

$$\mathbf{R} = \mathbf{T}\sigma^{-1}\mathbf{T}^{\dagger} = \mathbf{T}(\mathbf{T}^{\dagger}\mathbf{S}\mathbf{T})^{-1}\mathbf{T}^{\dagger}. \tag{47}$$

Since the matrix $\mathbf{T}$ has block-diagonal structure, all matrix multiplies that involve $\mathbf{T}$ can be performed block by block, resulting in time savings proportional to the number of blocks. With the utilization of block-by-block multiplication, the calculation of σ requires $2\Sigma_x^F(Nn_xo_x+On_xo_x)$ floating point operations (FLOPs) and, therefore, scales as F^2nno. We used Cholesky factorization to invert σ which, in principle, can be made linear in O with the use of sparsity of σ. Construction of $\mathbf{R}$ from $\mathbf{T}$ and σ^{-1} takes $2\Sigma_x^F(On_xo_x+Nn_xo_x)$ FLOPs and also scales as F^2nno. Thus, the overall density matrix construction scales as F^2nno. Compared to F^3nno for the conventional procedure, speedups of the order of F (i.e., proportional to system size) are expected in this part of the SCF MI algorithm for large systems.

The DIIS error matrix can be evaluated according to Eq. (39). However, matrix multiplications of $N\times N$ matrices $\mathbf{f}$, $\mathbf{R}$, and $\mathbf{S}$ scale cubically with N. In order to avoid N^3 steps we rewrite Eq. (39) as

$$\begin{aligned}[\mathbf{err}]_{xx} &= 2[\mathbf{S}]_{xx}[\mathbf{T}\sigma^{-1}\mathbf{T}^{\dagger}\mathbf{f}(\mathbf{T}\sigma^{-1}\mathbf{T}^{\dagger}\mathbf{S}-\mathbf{1})]_{xx} - \text{transpose}\\ &= 2[\mathbf{S}\mathbf{T}]_{xx}[(\sigma^{-1}(\mathbf{T}^{\dagger}\mathbf{f}\mathbf{T})\sigma^{-1})(\mathbf{T}^{\dagger}\mathbf{S})]_{xx}\\ &\quad - 2[\mathbf{S}\mathbf{T}]_{xx}[\sigma^{-1}(\mathbf{T}^{\dagger}\mathbf{f})]_{xx} - \text{transpose}.\end{aligned} \tag{48}$$

If the calculation of **err** is performed in the order specified by the parentheses, then the most expensive matrix multiplies, namely, $\mathbf{f}\times\mathbf{T}$ and $\mathbf{f}\mathbf{T}\times\sigma^{-1}$, scale as F^2nno and F^3noo, respectively. The total number of matrix multiplies is 9, and the maximum temporary double-precision storage is $3NO$. Therefore, the scaling of the overall DIIS error matrix evaluation, $\max(F^2nno, F^3noo)$, favorably compares with the conventional cubic scaling, which in terms of fragments is $4F^3nnn$. It is also worth noting that, unlike the previously proposed error vector,[34] error vector (48) does not require evaluation of the projected Fock matrix nor the effective overlap matrix (see next paragraph) and, therefore, is faster.

Blocks of the locally projected Fock matrix are built from the full Fock matrix in the current implementation of the SCF MI algorithm. In the case of the Gianinetti equations, the projected Fock matrix and the effective overlap matrix are computed according to the following equations:

$$\begin{aligned}[\mathbf{f}_G^x]_{xx} &= [\mathbf{f}]_{xx} - [(\mathbf{f}\mathbf{T})(\sigma^{-1}\mathbf{T}^{\dagger}\mathbf{S})]_{xx} - \text{transpose}\\ &\quad + [(\mathbf{S}\mathbf{T}\sigma^{-1})(\mathbf{T}^{\dagger}\mathbf{f}\mathbf{T})(\sigma^{-1}\mathbf{T}^{\dagger}\mathbf{S})]_{xx}\\ &\quad + [\mathbf{f}\mathbf{T}\sigma^{-1}]_{xx}[\sigma^{-1}\mathbf{T}^{\dagger}\mathbf{S}]_{xx} + \text{transpose}\\ &\quad - [(\mathbf{S}\mathbf{T}\sigma^{-1})(\mathbf{T}^{\dagger}\mathbf{f}\mathbf{T})\sigma^{-1}]_{xx}[\sigma^{-1}\mathbf{T}^{\dagger}\mathbf{S}]_{xx} - \text{transpose}\\ &\quad + [\mathbf{S}\mathbf{T}\sigma^{-1}]_{xx}[\sigma^{-1}(\mathbf{T}^{\dagger}\mathbf{f}\mathbf{T})\sigma^{-1}]_{xx}[\sigma^{-1}\mathbf{T}^{\dagger}\mathbf{S}]_{xx},\end{aligned} \tag{49}$$

$$\begin{aligned}[\mathbf{S}_G^x]_{xx} &= [\mathbf{S}]_{xx} - [(\mathbf{S}\mathbf{T})(\sigma^{-1}\mathbf{T}^{\dagger}\mathbf{S})]_{xx}\\ &\quad + [\mathbf{S}\mathbf{T}\sigma^{-1}]_{xx}[\sigma^{-1}\mathbf{T}^{\dagger}\mathbf{S}]_{xx}.\end{aligned} \tag{50}$$

For the Stoll equations, the projected Fock matrix and the effective overlap matrices are given by

$$\begin{aligned}[\mathbf{f}_S^x]_{xx} &= [\mathbf{f}]_{xx} - [(\mathbf{f}\mathbf{T})(\sigma^{-1}\mathbf{T}^{\dagger}\mathbf{S})]_{xx} - \text{transpose}\\ &\quad + [(\mathbf{S}\mathbf{T}\sigma^{-1})(\mathbf{T}^{\dagger}\mathbf{f}\mathbf{T})(\sigma^{-1}\mathbf{T}^{\dagger}\mathbf{S})]_{xx}\\ &\quad + [\mathbf{f}\mathbf{T}\sigma^{-1}]_{xx}[\mathbf{T}^{\dagger}\mathbf{S}]_{xx} + \text{transpose}\\ &\quad - [(\mathbf{S}\mathbf{T}\sigma^{-1})(\mathbf{T}^{\dagger}\mathbf{f}\mathbf{T})\sigma^{-1}]_{xx}[\mathbf{T}^{\dagger}\mathbf{S}]_{xx} - \text{transpose}\\ &\quad + [\mathbf{S}\mathbf{T}]_{xx}[\sigma^{-1}(\mathbf{T}^{\dagger}\mathbf{f}\mathbf{T})\sigma^{-1}]_{xx}[\mathbf{T}^{\dagger}\mathbf{S}]_{xx},\end{aligned} \tag{51}$$

$$[\mathbf{S}_S^x]_{xx} = [\mathbf{S}]_{xx}. \tag{52}$$

Again, we performed matrix multiplications in the order specified by the parentheses to achieve better scaling. Construction of both $\mathbf{f}_G^x$ and $\mathbf{S}_G^x$ matrices requires 17 matrix multiplications and $3NO+OO+2Nn$ words of double-precision temporary storage. $\mathbf{f}_S^x$ and $\mathbf{S}_S^x$ can be computed with 12 matrix multiplications and $3NO+2Nn$ words of temporary storage memory. However, in both cases the most expensive multiplies scale as $\max(F^2nno, F^3noo)$. All the multiplies that can be skipped in calculations with the Stoll method are inexpensive and will not lead to significant time savings relative to the Gianinetti method. In principle, the amount of temporary storage can be further decreased to NO, but this will compromise the speed of the calculations.

The formation of the locally projected Fock matrix of Nagata requires inversion of the MO overlap matrices $\sigma_{\Theta x}$ individually for each fragment. The calculation of F inverse matrices $(O-o_x)\times(O-o_x)$ scales as F^4ooo. Therefore, the algorithm based on the SCF MI equations of Nagata becomes inferior to the locally projected formalism of Stoll and Gianinetti for systems with large numbers of fragments. Making some approximations to the MO overlap matrix can improve the overall scaling of the Nagata method,[29] but we will not consider this approach further here.

The subsequent diagonalization of the diagonal blocks of the projected Fock matrix scales as $Fnnn$ (i.e., linearly with the number of fragments) and therefore does not represent the bottleneck of the SCF MI iterative procedure. It is worth noting that parallelization of the SCF MI is straightforward and is expected to be very efficient.

B. SCF MI(ARS) and SCF MI(RS) algorithms

The implementation of the second-order perturbative correction is relatively simple. First, we orthogonalize the ALMOs using inverse Cholesky factors ($\mathbf{L}$) of the full MO overlap matrix σ_{NN},

$$\sigma_{NN} = \mathbf{L}\mathbf{L}^{\dagger}, \tag{53}$$

$$\mathbf{C}_0 = \mathbf{C}_{\mathrm{MI}}(\mathbf{L}^{-1})^{\dagger}. \tag{54}$$

The lower triangular structure of $\mathbf{L}^{-1}$ guarantees invariance of the occupied subspace given that the occupied orbitals are represented by the first O columns of $\mathbf{C}_{\mathrm{MI}}$. $\mathbf{C}$, $\mathbf{T}$, are $\mathbf{V}$ are MO coefficient matrices for all, occupied, and virtual orbitals, respectively.

The Fock matrix in the basis of orthogonalized MO orbitals is calculated from the converged SCF MI Fock matrix $\mathbf{f}(\mathbf{R}_{\mathrm{MI}})$,

$$\mathbf{f}_0 = \mathbf{C}_0^{\dagger}\mathbf{f}(\mathbf{R}_{\mathrm{MI}})\mathbf{C}_0. \tag{55}$$

The diagonalization of the occupied-occupied and virtual-virtual blocks yields orthogonalized pseudocanonical MOs $|\bar{\psi}_q\rangle$,

$$[\mathbf{f}_0]_{\mathrm{OO}}\mathbf{T} = \mathbf{T}\bar{\boldsymbol{\epsilon}}_O, \tag{56}$$

$$[\mathbf{f}_0]_{\mathrm{VV}}\mathbf{V} = \mathbf{V}\bar{\boldsymbol{\epsilon}}_V, \tag{57}$$

with a coefficient matrix given by

$$\bar{\mathbf{C}} = \mathbf{C}_0(\mathbf{T} \oplus \mathbf{V}). \tag{58}$$

The Fock matrix in the pseudocanonical basis,

$$\bar{\mathbf{f}} = (\mathbf{T} \oplus \mathbf{V})^{\dagger}\mathbf{f}_0(\mathbf{T} \oplus \mathbf{V}), \tag{59}$$

is used to calculate the energy correction according to Eq. (44) and the correction to the orbitals according to Eq. (45). The matrix equations for the corrected occupied orbitals $\bar{\mathbf{T}}^c$ and the corrected density matrix $\mathbf{R}^c$ are

$$\bar{\mathbf{T}}^c = \bar{\mathbf{V}}\mathbf{M}, \tag{60}$$

$$\mathbf{R}^c = \bar{\mathbf{T}}^c(\bar{\mathbf{T}}^{c\dagger}\mathbf{S}\bar{\mathbf{T}}^c)^{-1}\bar{\mathbf{T}}^{c\dagger}, \tag{61}$$

where elements of $V \times O$ $\mathbf{M}$ matrix are $M_{ai} = \bar{f}_{ai}/(\bar{\epsilon}_i - \bar{\epsilon}_a)$.

The most computationally expensive steps of this SCF MI(ARS) algorithm are the evaluation of the Fock matrix in the orthogonalized (55) and pseudocanonical (59) MO representations, as well as the diagonalization of the virtual-virtual block of $\mathbf{f}_0$ (57) and the formation of the perturbed density matrix $\mathbf{R}^c$ (61). These steps scale as N^3, NV^2, V^3, and N^3, respectively.

The infinite-order perturbative correction [SCF MI(RS)] is obtained by full diagonalization of the final converged Fock matrix $\mathbf{f}(\mathbf{R}_{\mathrm{MI}})$ in the last iteration of the SCF MI procedure (an N^3 step). The corrected density matrix is then constructed from the orthogonal eigenvectors of $\mathbf{f}(\mathbf{R}_{\mathrm{MI}})$ (an N^3 step). The energy correction is calculated according to Eq. (46) (an N^2 step). The infinite-order correction can serve as an indicator of the convergence of the perturbation expression and does not contain steps that scale higher than N^3.

IV. RESULTS AND DISCUSSION

The Hartree–Fock method and density functional theory with the EDF1 functional[43] were used to test the performance of the locally projected methods for water clusters.

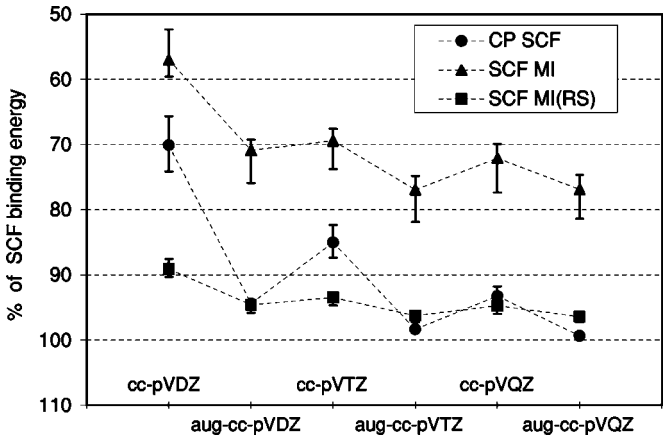

FIG. 1. Percent of the full SCF binding energy recovered in with the CP SCF, SCF MI, and SCF MI(RS) methods for small water clusters.

Each water molecule was considered as a separate fragment. All energies were calculated with a development version of the Q-CHEM software package.[42] Linear-scaling algorithms were employed for the formation of the Fock matrix.[12,13,15,16,19] The integral threshold was set to 10^{-8}. The DIIS criterion for SCF convergence was taken to be 10^{-5}.

A. Accuracy of the locally projected methods

HF calculations were carried out for water dimers, trimers, tetramers, pentamers, and hexamers with gradually increasing basis set sizes (cc-pVDZ, aug-cc-pVDZ, cc-pVTZ, aug-cc-pVTZ, cc-pVQZ, and aug-cc-pVQZ). The structures of the clusters were optimized at the HF/cc-pVDZ level of theory. The calculated binding energies for the full SCF, counterpoise corrected (CP) SCF, SCF MI, SCF MI(ARS), and SCF MI(RS) are given in Table I. Figure 1 shows the average percentage of the full SCF binding energy recovered with the CP SCF, SCF MI, and SCF MI(RS) methods. The error bars in Fig. 1 indicate the spread in the recovered energies for clusters of different size (dimer-hexamer).

Our calculations closely reproduce the energies obtained by Nagata *et al.*[29] (Table II in the original paper) for the SCF, CP SCF, and SCF MI methods. The large BSSE obtained for calculations done with cc-pVXZ basis sets is significantly reduced by addition of diffuse functions, i.e., in aug-cc-pVXZ the BSSE is around 1% of the binding energy (Fig. 1). It has been observed previously[29] that the performance of the SCF MI method in terms of the full SCF binding energy recovery increases as the basis set approaches completeness (Fig. 1). However, even for essentially complete sets, such as aug-cc-pVQZ (BSSE is less than 1%), the percentage of the binding energy recovered is still very low (75%–82%). This relatively poor behavior of the SCF MI method must be attributed to the loss of variational degrees of freedom in the constrained MOs (1). The excluded degrees of freedom are associated with charge transfer between the fragments as well as with BSSE. Since charge transfer contributes significantly to the hydrogen bonding in water clusters[3] the SCF MI energies are higher than the CP SCF energies. Therefore, the SCF MI theory can only be reliably applied to systems in

TABLE I. Binding energies (kcal/mol) for small water clusters.

		Dimer	Trimer	Tetramer	Pentamer	Hexamer
cc-pVDZ						
	SCF	−5.78	−17.57	−29.89	−39.01	−47.10
	CP SCF	−3.87	−11.54	−21.10	−28.49	−34.93
	SCF MI	−3.44	−9.20	−16.62	−22.62	−28.06
	SCF MI(ARS)	−5.22	−15.40	−26.49	−34.85	−42.32
	SCF MI(RS)	−5.22	−15.39	−26.47	−34.84	−42.29
aug-cc-pVDZ						
	SCF	−3.88	−11.44	−20.74	−27.67	−33.64
	CP SCF	−3.67	−10.73	−19.59	−26.21	−31.85
	SCF MI	−2.95	−8.04	−14.37	−19.16	−23.47
	SCF MI(ARS)	−3.72	−10.82	−19.53	−26.05	−31.72
	SCF MI(RS)	−3.72	−10.82	−19.53	−26.04	−31.71
cc-pVTZ						
	SCF	−4.46	−13.37	−23.63	−31.25	−37.80
	CP SCF	−3.68	−11.10	−20.23	−27.13	−33.03
	SCF MI	−3.30	−9.07	−15.97	−21.35	−26.31
	SCF MI(ARS)	−4.23	−12.42	−21.99	−29.16	−35.40
	SCF MI(RS)	−4.23	−12.41	−21.98	−29.15	−35.40
aug-cc-pVTZ						
	SCF	−3.70	−10.90	−20.00	−26.84	−32.65
	CP SCF	−3.63	−10.70	−19.68	−26.43	−32.17
	SCF MI	−3.03	−8.45	−14.98	−20.09	−24.68
	SCF MI(ARS)	−3.60	−10.50	−19.18	−25.73	−31.34
	SCF MI(RS)	−3.60	−10.50	−19.18	−25.73	−31.34
cc-pVQZ						
	SCF	−4.00	−11.84	−21.38	−28.52	−34.62
	CP SCF	−3.68	−10.93	−20.02	−26.85	−32.67
	SCF MI	−3.10	−8.56	−14.97	−19.95	−24.54
	SCF MI(ARS)	−3.84	−11.21	−20.16	−26.89	−32.72
	SCF MI(RS)	−3.84	−11.21	−20.16	−26.89	−32.72
aug-cc-pVQZ						
	SCF	−3.70	−10.87	−19.95	−26.77	−32.58
	CP SCF	−3.67	−10.79	−19.83	−26.62	−32.40
	SCF MI	−3.01	−8.43	−14.89	−20.04	−24.74
	SCF MI(ARS)	−3.59	−10.50	−19.15	−25.72	−31.37
	SCF MI(RS)	−3.59	−10.50	−19.15	−25.72	−31.36

which charge-transfer effects between components are negligible and interactions are purely electrostatic.

For systems with non-negligible charge-transfer effects perturbative corrections can provide a good approximation to the full SCF energies. Unfortunately the perturbation also reintroduces BSSE into the interaction energy. Thus, the SCF MI(RS) energies can be lower than the CP SCF energies especially for small basis sets (Fig. 1).

As seen from Table I the binding energies obtained with the SCF MI(ARS) and SCF MI(RS) perturbation methods do not differ more than 0.01 kcal/mol per hydrogen bond. The fourth-order energy correction on water clusters (not shown here) is in general less than 0.1% of the second-order correction. Therefore, we conclude that the perturbation expansion is satisfactorily converged at second order for water clusters with molecules around their equilibrium distances from each other.

The SCF MI(RS) method recovers as much as 96%–97% of the full SCF binding energy in large basis sets (aug-cc-pVTZ and aug-cc-pVQZ). For small basis sets such as cc-pVDZ the performance of the corrected methods is worse (90% of the full SCF binding energies) and additional care must be taken to remove the reintroduced BSSE.

To test how the quality of results depends on the distance between water molecules, potential energy curves were generated for the water dimer at the HF/aug-cc-pVDZ level. All geometric parameters other than the O–O distance were fixed at the MP2/aug-cc-pVDZ minimum energy structure. Results of the SCF MI and SCF MI(RS) methods were compared with the conventional SCF energies and the CP SCF energies (Fig. 2). Figure 2 shows that the SCF MI method reproduces only 81% of the full SCF binding energy (85% of the CP SCF energy) and gives a larger minimum energy O–O distance whereas the corrected methods significantly improve the energies: SCF MI(ARS) and SCF CP curves almost coincide at all distances. Our results reproduce those obtained

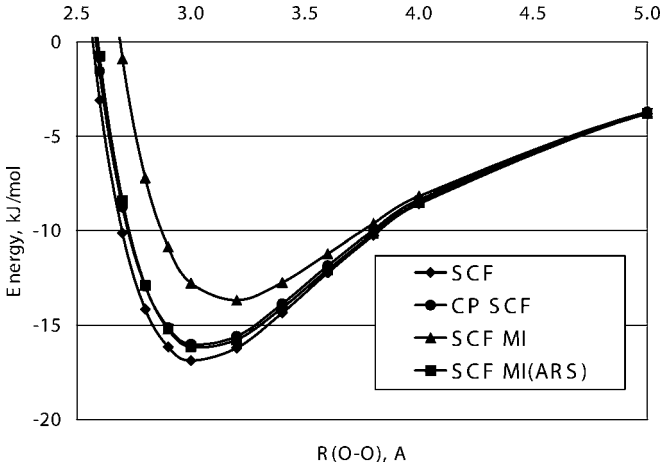

FIG. 2. Potential energy curve for water dimer, HF/aug-cc-pVDZ.

by Nagata *et al.* and confirm that our SCF MI(ARS) formalism is equivalent to the LP SE MP2 published previously,[36] despite the very different form of the working equations.

Summarizing, the test calculations on small water clusters show that in order to obtain accurate SCF interaction energies, the single Roothaan step perturbative method should be used after the SCF MI iterative procedure. Large basis sets are desirable to obtain accurate energies. As we will show in Sec. IV B the computational advantage of the SCF MI method grows with basis set size.

B. Convergence and computational efficiency of the locally projected methods

As discussed in the Introduction, each SCF iteration can be represented as a sequence of two steps. On the first step the Fock matrix is constructed from the density matrix (we denote this step as DM2F); on the next step a new density matrix is obtained from the constructed Fock matrix (F2DM). The second step traditionally includes three components: the DIIS extrapolation of the Fock matrix (DIISX), the diagonalization of the extrapolated Fock matrix (F2MO), and the construction of the density matrix from the newly obtained MOs (MO2DM). As mentioned before, we use the SCF MI method to remove the bottleneck associated with the second step, F2DM. In this subsection we present the speedups achieved by replacing three parts of the conventional F2DM step with their SCF MI equivalents. The speedup is defined simply as the ratio of the time necessary to perform computation in the conventional SCF algorithm to the time taken by the SCF MI algorithm. The speedups predicted from counting FLOPs are $(n/o)^2$ for the DIISX and F2MO routines (see Sec. III), and F for the MO2DM.

Table II summarizes speedups for all three routines in calculations on large two-dimensional water clusters in 6-31$g(d,p)$ basis set $[(n/o)^2=25]$. It can be seen that the speedups achieved for DIISX and F2MO are larger than the predicted factor of 25 even for systems of moderate size (several hundred basis set functions). This effect can be explained by improved CPU cache effectiveness when performing small block-by-block matrix multiplications in DIISX. Smaller blocks are more likely to fit into the CPU cache which further increases the relative speed of the SCF MI algorithm. For large matrices in the SCF routines a significant amount of time is spent loading-unloading cache data. In the case of the F2MO routine large speedups are explained by the large prefactors in the conventional diagonalization code. The speedups in the case of MO2DM are lower than predicted since the prediction does not take into account time spent for σ inversion. Although the inversion scales only as O^3, it has a large prefactor and becomes negligible only for very large systems.

TABLE II. Speedups for 6-31$g(d,p)$ calculations on large water clusters. Results are the same for both HF and EDF1 calculations.

No. of molecules	Basis set size, N	Routine				
		DIISX	F2MO	MO2DM	**F2DM**	Overall[a]
9	225	8.50	11.33	1.00	**7.57**	0.84
18	450	35.00	34.73	1.80	**27.65**	1.05
36	900	58.03	67.02	4.48	**50.02**	1.45
72	1800	105.26	95.37	7.38	**80.50**	2.81
144	3600	125.10	102.55	12.59	**97.13**	5.63
288	7200	172.59	104.83	15.79	**108.26**	8.20

[a]For EDF1/6-31$g(d,p)$ calculations.

The combined speedup for the F2DM step is also shown in Table II. For 144 water molecules the speedup for this step is about two orders of magnitude. Figure 3 represents the relative amounts of time spent in the Fock formation (DM2F) and the diagonalization (F2DM) routines for both SCF and SCF MI iterations. For large systems most of the CPU time in the conventional SCF code is spent for the diagonalization (98% for the diagonalization, $N=7200$), while in the SCF MI code the Fock formation remains the limiting step for these systems (73% for the Fock formation, $N=7200$). Therefore, the SCF MI algorithm removes the diagonalization bottleneck for calculations on large systems containing multiple fragments. As predicted from counting FLOPs, speedups for the diagonalization increase with the size of the basis set. For example, the diagonalization speedups for the water hexamer are 6.3, 17.0, and 25.4 in aug-cc-

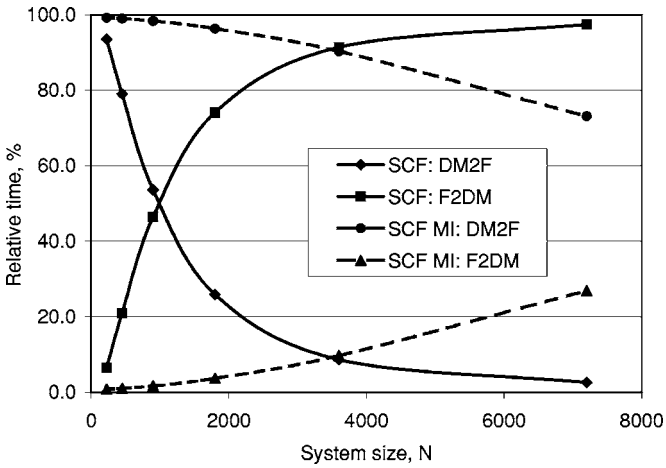

FIG. 3. Percent of iteration time spent in Fock build and diagonalization for SCF (solid lines) and SCF MI (dashed lines) iterations. Large water clusters, EDF1/6-31$g(d,p)$.

TABLE III. Average number of SCF iterations for water clusters containing 9–288 molecules; 6-31$g(d,p)$ basis sets.

Method	Gianinetti SCF MI	Stoll SCF MI	Gianinetti SCF MI	Stoll SCF MI	SCF	SCF
Acceleration	DIIS	DIIS	none	none	DIIS	DIIS
Initial guess	SMO	SMO	SMO	SMO	SAD	SMO
HF	6–7	7	9–10	10	7–8	5–6
EDF1	7	7	>30	>30	8–17	6

pVDZ, aug-cc-pVTZ, and aug-cc-pVQZ, respectively. Thus, the SCF MI method is computationally effective for large basis set calculations.

It is remarkable that some speedup can be achieved in the formation of the Fock matrix (DM2F) without any modification of the algorithms or code used for this step. For example, the time spent for the exchange matrix construction in the HF/cc-pVDZ calculations is decreased by roughly a factor of 2 (using the LinK algorithm[19]) just by virtue of using the SCF MI density matrices. The Coulomb matrix is also evaluated faster with the SCF MI density in HF calculations (speedups are approximately a factor of 1.5). This improvement is due to the fact that these linear-scaling algorithms for the Fock formation exploit the locality of the orbitals that are used to construct $\mathbf{f}$.[12,13,15,16,19] Therefore, the absolutely localized orbitals produced in the SCF MI method give some improvement for this step, because they are giving a density matrix that is more strongly localized than is the case in conventional SCF calculations on the same systems.

The efficiency of the proposed DIIS extrapolation scheme is illustrated in Table III. As one can see, the number of iterations in the SCF MI procedure is decreased significantly when DIIS extrapolation is used. Comparison of the DIIS-accelerated SCF MI with the conventional DIIS-accelerated SCF calculation shows that the number of SCF MI iterations is smaller than the number of conventional SCF iterations, particularly for the EDF1 functional. The reason for the faster convergence of the SCF MI procedure is the high quality of the initial guess [generated as a superposition of the converged orbitals on isolated fragments (SMO)]. When the conventional SCF is performed with the SMO guess instead of the superposition of the atomic densities (SAD) guess, a large number of iterations can be saved (Table III), especially with the EDF1 functional. The generation of the SMO initial guess is rapid compared to the iteration time, and is a useful alternative to the SAD guess. In combination with DIIS extrapolation, this makes the SCF MI method a practical tool for calculations on large systems of the weakly interacting fragments. Finally, one can see from Table III that the locally projected equations of Stoll require approximately the same number of steps as the equations of Gianinetti. Both formulations converge to the same result and take the same CPU time.

As mentioned before, both SCF MI(ARS) and SCF MI(RS) give essentially the same energies and do not contain steps that scale higher than N^3. However, the SCF MI(ARS) needs approximately twice as much time as the SCF MI(RS) algorithm in all test calculations due to the need for numerous matrix multiplications and several diagonalizations (53)–(61). Therefore, the SCF MI(RS) is more practical and should be used to perform corrections to the energy and to the orbitals after the SCF MI iterative procedure.

The last column of Table II shows the speedups for the entire computation for water clusters of different sizes using the HF/6-31$g(d,p)$ SCF MI(RS) method. The overall speedup is approximately one order of magnitude for the 6-31$g(d,p)$ basis set, and is expected to be higher for larger basis sets. The overall speedup is not as high as the speedup for the diagonalization step, since a significant amount of time is still spent for the Fock formation and in the last Fock diagonalization for SCF MI(RS) correction. Therefore, fast methods for the Fock construction that take into account the block-diagonal structure of the constrained MO orbitals are desirable to further exploit the potential of the SCF MI approach.

V. CONCLUSIONS

In this paper, we have revisited a locally projected self-consistent field method for molecular interactions (SCF MI), which is appropriate for molecular clusters and liquids. The central approximation in SCF MI is to expand molecular orbitals (MOs) of a given fragment in terms of only the atomic orbitals (AOs) that are on atoms in that fragment. This leads to absolutely localized MOs (ALMOs) that are free from basis set superposition errors (BSSE), but that also prevent charge transfer between fragments. Our main conclusions are as follows:

(1) Our formulation and implementation are the first to explicitly take advantage of the computational savings that are possible in this approach. Additionally we have presented a simple formulation of a correction for charge-transfer effects that is based on performing one final diagonalization of the Fock matrix obtained from a converged SCF MI calculation.

(2) As was known previously, SCF MI cannot quantitatively reproduce the results of full SCF calculations for hydrogen bond energies of water clusters in even large basis sets. However, good accuracy is achieved if the SCF MI iteration scheme is combined with the charge-transfer perturbative correction [SCF MI(RS)] in large basis set calculations. Comparison of energies with and without correction allows extraction of electrostatic and charge-transfer contributions to intermolecular interaction energies.

(3) The computational advantage of SCF MI over the conventional SCF method grows with both basis set size and number of fragments. Although still cubic scaling, SCF MI effectively removes the diagonalization step as a bottleneck in these calculations, because it contains such a small prefactor. In combination with the single step correction, substantial speedups are obtained.

(4) The combination of good accuracy with substantial computational advantage suggests that SCF MI(RS) could be valuable for first principles studies of potential surfaces (and possibly to drive dynamics on those sur-

faces) of large clusters, and nanosolvation by such clusters, as well as possibly studies of liquids and solutions.

A number of follow-on research developments appear useful based on this work. The development of specialized algorithms to construct the Fock matrix exploiting the block structure of the ALMOs is one example, while the formulation and implementation of the analytical gradient of the charge-transfer corrected energy expression is a second example.

[1] A. W. Castleman, Chem. Rev. (Washington, D.C.) **94**, 1721 (1994).
[2] J.-M. Lehn, *Supramolecular Chemistry: Concepts and Perspectives* (Weinheim, New York, 1995).
[3] G. A. Jeffrey, *An Introduction to Hydrogen Bonding* (Oxford University Press, Oxford, 1997).
[4] S. Scheiner, *Hydrogen Bonding: A Theoretical Perspective* (Oxford University Press, Oxford, 1997).
[5] F. N. Keutsch, J. D. Cruzan, and R. J. Saykally, Chem. Rev. (Washington, D.C.) **103**, 2533 (2003).
[6] S. S. Xantheas and T. H. Dunning, Jr., Adv. Mol. Vib. Collision Dyn. **3**, 281 (1998).
[7] R. Ludwig, Angew. Chem., Int. Ed. **40**, 1808 (2001).
[8] M. E. Tuckerman, P. J. Ungar, T. von Rosenvinge, and M. L. Klein, J. Phys. Chem. **100**, 12878 (1996).
[9] M. E. Tuckerman, J. Phys.: Condens. Matter **14**, R1297 (2002).
[10] A. Szabo and N. S. Ostlund, *Modern Quantum Chemistry: Introduction to Advanced Electronic Structure Theory* (Dover, Mineola, NY, 1996).
[11] R. G. Parr and W. Yang, *Density-Functional Theory of Atoms and Molecules* (Oxford University Press, Oxford, 1989).
[12] C. A. White, B. G. Johnson, P. M. W. Gill, and M. Head-Gordon, Chem. Phys. Lett. **230**, 8 (1994).
[13] C. A. White, B. G. Johnson, P. M. W. Gill, and M. Head-Gordon, Chem. Phys. Lett. **253**, 268 (1996).
[14] M. C. Strain, G. E. Scuseria, and M. J. Frisch, Science **271**, 51 (1996).
[15] C. A. White and M. Head-Gordon, J. Chem. Phys. **104**, 2620 (1996).
[16] Y. Shao and M. Head-Gordon, Chem. Phys. Lett. **323**, 425 (2000).
[17] L. Fusti-Molnar and J. Kong, J. Chem. Phys. **122**, 74108 (2005).
[18] E. Schwegler, M. Challacombe, and M. Head-Gordon, J. Chem. Phys. **106**, 9708 (1997).
[19] C. Ochsenfeld, C. A. White, and M. Head-Gordon, J. Chem. Phys. **109**, 1663 (1998).
[20] J. M. Perez-Jorda and W. Yang, Chem. Phys. Lett. **241**, 469 (1995).
[21] R. E. Stratmann, G. E. Scuseria, and M. J. Frisch, Chem. Phys. Lett. **257**, 213 (1996).
[22] Y. H. Shao, C. A. White, and M. Head-Gordon, J. Chem. Phys. **114**, 6572 (2001).
[23] S. Goedecker, Rev. Mod. Phys. **71**, 1085 (1999).
[24] G. E. Scuseria, J. Phys. Chem. A **103**, 4782 (1999).
[25] D. R. Bowler, T. Miyazaki, and M. J. Gillan, J. Phys.: Condens. Matter **14**, 2781 (2002).
[26] P. E. Maslen, C. Ochsenfeld, C. A. White, M. S. Lee, and M. Head-Gordon, J. Phys. Chem. A **102**, 2215 (1998).
[27] E. Gianinetti, I. Vandoni, A. Famulari, and M. Raimondi, Adv. Quantum Chem. **31**, 251 (1998).
[28] E. Gianinetti, M. Raimondi, and E. Tornaghi, Int. J. Quantum Chem. **60**, 157 (1996).
[29] T. Nagata, O. Takahashi, K. Saito, and S. Iwata, J. Chem. Phys. **115**, 3553 (2001).
[30] J. M. Cullen, Int. J. Quantum Chem., Quantum Chem. Symp. **25**, 193 (1991).
[31] H. Stoll, G. Wagenblast, and H. Preuss, Theor. Chim. Acta **57**, 169 (1980).
[32] P. Pulay, Chem. Phys. Lett. **73**, 393 (1980).
[33] P. Pulay, J. Comput. Chem. **3**, 556 (1982).
[34] A. Famulari, G. Calderoni, F. Moroni, M. Raimondi, and P. B. Karadakov, J. Mol. Struct.: THEOCHEM **549**, 95 (2001).
[35] A. Hamza, A. Vibok, G. J. Halasz, and I. Mayer, THEOCHEM **501–502**, 427 (2000).
[36] T. Nagata and S. Iwata, J. Chem. Phys. **120**, 3555 (2004).
[37] M. Head-Gordon, P. E. Maslen, and C. A. White, J. Chem. Phys. **108**, 616 (1998).
[38] M. Head-Gordon, J. Phys. Chem. **100**, 13213 (1996).
[39] M. Head-Gordon, Y. Shao, C. Saravanan, and C. A. White, Mol. Phys. **101**, 37 (2003).
[40] W. Liang and M. Head-Gordon, J. Phys. Chem. A **108**, 3206 (2004).
[41] M. S. Lee and M. Head-Gordon, Comput. Chem. (Oxford) **24**, 295 (2000).
[42] J. Kong, C. A. White, A. I. Krylov *et al.*, J. Comput. Chem. **21**, 1532 (2000).
[43] R. D. Adamson, P. M. W. Gill, and J. A. Pople, Chem. Phys. Lett. **284**, 6 (1998).